Video Article

Universal Hand-held Three-dimensional Optoacoustic Imaging Probe for Deep Tissue Human Angiography and Functional Preclinical Studies in Real Time

Xosé Deán-Ben[1], Thomas Felix Fehm[1,2], Daniel Razansky[1,2]

[1]Institute for Biological and Medical Imaging (IBMI), Helmholtz Zentrum München

[2]Faculty of Medicine, Technische Universität München

Correspondence to: Daniel Razansky at dr@tum.de

URL: https://www.jove.com/video/51864
DOI: doi:10.3791/51864

Keywords: Physiology, Issue 93, Optoacoustic tomography, photoacoustic imaging, hand-held probe, volumetric imaging, real-time tomography, five dimensional imaging, clinical imaging, functional imaging, molecular imaging, preclinical research

Date Published: 11/4/2014

Citation: Deán-Ben, X., Fehm, T.F., Razansky, D. Universal Hand-held Three-dimensional Optoacoustic Imaging Probe for Deep Tissue Human Angiography and Functional Preclinical Studies in Real Time. *J. Vis. Exp.* (93), e51864, doi:10.3791/51864 (2014).

Abstract

The exclusive combination of high optical contrast and excellent spatial resolution makes optoacoustics (photoacoustics) ideal for simultaneously attaining anatomical, functional and molecular contrast in deep optically opaque tissues. While enormous potential has been recently demonstrated in the application of optoacoustics for small animal research, vast efforts have also been undertaken in translating this imaging technology into clinical practice. We present here a newly developed optoacoustic tomography approach capable of delivering high resolution and spectrally enriched volumetric images of tissue morphology and function in real time. A detailed description of the experimental protocol for operating with the imaging system in both hand-held and stationary modes is provided and showcased for different potential scenarios involving functional and molecular studies in murine models and humans. The possibility for real time visualization in three dimensions along with the versatile handheld design of the imaging probe make the newly developed approach unique among the pantheon of imaging modalities used in today's preclinical research and clinical practice.

Video Link

The video component of this article can be found at https://www.jove.com/video/51864/

Introduction

Optoacoustic (photoacoustic) imaging attracts growing interest from the biological and medical research communities, as manifested by the ever increasing number of publications encompassing variety of new applications that exploit the unique advantages offered by the technology [1-5]. In particular, the capacity to image spectrally distinctive photo-absorbing agents with high spatio-temporal resolution at depths far beyond the diffusive limit of light opens unprecedented capabilities for functional and molecular imaging [6-10].

Indeed, translation of the optoacoustic technology into clinical practice comes with promising prospects in diagnostics and treatment monitoring of many diseases. Yet, the limited propagation of photons in optically scattering and absorbing tissues and the generally weak responses associated with the optoacoustic phenomenon limit the applicable depth of the method. As a result, hand-held optoacoustic probes have been attempted to image parts accessible from outside of the body [11,12] while endoscopic systems are used to provide images from within the body by inserting them via natural orifices [13]. Some low absorbing parts of human body, such as female breast, are also accessible by tomographic optoacoustic scanners [14,15]. Of particular interest is the hand-held approach as it enables large versatility, similarly to ultrasonography. Here, adaptation of the common ultrasound linear array probes for optoacoustic imaging remains challenging, mainly due to fundamental differences in tomographic imaging requirements between ultrasound and optoacoustics. While high frame rates in standard ultrasonography are enabled by sequential transmit-receive schemes employing high pulse repetition frequencies in the kHz range, real-time three-dimensional optoacoustic imaging is achieved by simultaneous collection of volumetric tomographic data from a single interrogating laser pulse. Thus, high quality optoacoustic imaging implies acquisition of three-dimensional data from the largest possible solid angle around the imaged object.

Recently, we introduced the first handheld optoacoustic probe for three-dimensional (volumetric) imaging in real time[16]. The system is based on a two-dimensional array of 256 piezoelectric elements arranged upon a spherical surface (blue dots in **Figure 1A**) covering an angle of 90°. The size of the individual elements of approximately 3 x 3 mm^2, as well as their orientation and frequency bandwidth (approximately 2-6 MHz) guarantee effective signal collection from a centimeter-scale volume surrounding the center of the sphere (black cube in **Figure 1A**). Optical excitation of the imaging region is provided with a fiber bundle inserted through a central cylindrical cavity of the array, so that any wavelength susceptible of being transmitted through the fiber bundle can be used for imaging. An actual picture of the array of transducers along with the optical fiber bundle is shown in **Figure 1B**. The efficient excitation and simultaneous detection of signals allows deep-tissue imaging with single-shot excitation (one laser pulse), so that real-time imaging at a frame rate determined by the pulse repetition frequency of the laser is further enabled with a graphics-processing-unit (GPU) implementation of the reconstruction procedure [17]. A cylindrical casing with a transparent polyethylene membrane (**Figure 1C**) is attached to the transducer array to enclose an acoustically transmitting liquid medium (water). The

membrane is further coupled to the tissue by means of acoustic gel. A picture of the optoacoustic probe as being used in hand-held operation mode is shown in **Figure 1D**.

The demonstrated three dimensional hand-held optoacoustic imaging combined with the real time functional imaging capacity come with important advantages for clinical diagnostics and a number of potential applications are envisioned for various indications, such as peripheral vascular disease, lymphatic system disorders, breast cancer, skin lesions, inflammation or arthritis [18]. Furthermore, the fast imaging capacity enables visualization of dynamic biological events with the probe arranged in a stationary position. Combined with fast wavelength-tuning optical parametric oscillator (OPO) laser technology, this approach allows for real-time imaging of biodistribution of photo-absorbing agents. Thereby, new possibilities may equally emerge in small animal imaging applications, *e.g.*, in studying tissue hemodynamics, *in vivo* cell tracking, visualization of pharmacokinetics, organ perfusion, targeted molecular imaging of tumors and cardiovascular system, or neuroimaging.

In this work we provide a detailed description of the experimental imaging protocol to operate with the spherical array optoacoustic hand-held probe and showcase performance in several typical clinical and small animal imaging scenarios.

Protocol

The detailed procedure for operating with the volumetric hand-held optoacoustic probe is described below. This procedure is performed according to approved institutional regulations regarding animal and human experiments.

1. System Preparation

1. Switch on the laser for a warm-up period of ~15 min prior to operation for stabilizing the output light beam.
2. Place the water enclosing part with the isolating membrane that is in contact with the skin (**Figure 1**).
   NOTE: The distance between the isolating membrane (in contact with the skin) and the region with maximum sensitivity of the transducer (center of the spherical probe) establishes the effective imaging depth.
3. Fill the whole volume of approximately 100 ml between the isolating membrane and the surface of the transducer with deionized water by means of a pump.
4. Ensure that no water leakage nor air bubbles are present. Alternatively, avoid air bubbles by providing recirculation of water.
5. Perform the experiments at RT and ensure the coupling medium (water) is maintained at this temperature.

2. Imaging Preparation

1. Human imaging preparation.
2. Remove hair from the to-be-imaged part with a depilation lotion in order to avoid an undesired background in the images (this step is optional).
3. Apply ultrasound gel onto the skin around the region to be imaged in order to provide efficient acoustic coupling. Place the optoacoustic probe in the region of interest. Ensure that no air bubbles are present in the ultrasound coupling gel.
4. Animal imaging preparation.
5. Ensure that the care and experimental procedures with animals are in agreement with institutional and government rules and regulations.
6. Remove the fur of the animal in the region to be imaged with a shaving lotion. Protect the eyes of the animal with vet ointment, which prevents dryness and damage from exposure to intense pulsed laser radiation.
7. Anesthetize the animal by using intraperitoneal injection (IP) of ketamine/xylazine (100 mg/kg KG Ketamine + 5 mg/kg KG Xylazine) prior to the experiment or use isoflurane anesthesia (2-3 % (by volume) with 0.9 l/min gas flow) during the experiment. Confirm anesthetization by checking the reflex of the hind limb of the animal.
8. Apply ultrasound gel onto the skin around the region to be imaged in order to provide efficient acoustic coupling and place the optoacoustic probe in the region of interest. Ensure that no air bubbles are present in the ultrasound coupling gel.

3. Pre-view Operation Mode

1. Establish the imaging wavelength(s) between 690 nm and 900 nm and the pulse repetition rate between 10 and 50 Hz. Select the parameters for the acoustic data acquisition system – 1 MΩ input impedance. Acquire 2030 samples for each laser pulse at a sampling rate of 40 megasamples per second and 12 bit vertical resolution. Trigger the acquisition with Q-switch output of the laser.
2. Ensure that both the operator and the patient use protective goggles adapted to the optical excitation wavelength(s). Set the laser power so that the light fluence at the tissue surface is maintained below 20 mJ/cm^2 during the experiment for near-infrared wavelengths in order to satisfy safety exposure limits for human experiments[19] and to prevent thermal strain and skin damage in animals.
3. Start the pre-view software with a GPU implementation of processing algorithms to allow visualizing three-dimensional images at a frame rate corresponding to the pulse repetition rate of the laser.
4. Move the probe and/or the object to be imaged in order to optimize visualization performance and localize the structures of interest.

4. Data Acquisition

1. Data acquisition for scanning (hand-held) mode.
2. If necessary, inject a contrast agent prior to acquisition to enrich the contrast in the region of interest.
   NOTE: In our experiments we have not performed contrast-enhanced human imaging. Yet, various contrast agents can be potentially used for this purpose. Indocyanine Green (ICG) is one example of clinically-approved optical contrast agent that can be used for contrast enhancement at maximal recommended dose of 2 mg/kg of body weight in adults.

3. Start the hardware for data acquisition with the parameters described in 3.1 maintaining the execution of the preview software. Gently move the probe around the imaged region to track the structures of interest.
   NOTE: When images at multiple laser wavelengths are acquired simultaneously, the speed of probe motion in the hand-held mode has to be decreased significantly (preferably below 2 mm/sec for a laser pulse repetition rate of 50 Hz) in order to avoid motion-related artifacts in the spectrally unmixed images.
4. Data acquisition for stationary mode.
5. Mount the imaged object (*e.g.*, animal) and the hand-held probe onto the holder and start the acquisition with the parameters described in 3.1 maintaining the execution of the pre-view software.
6. Maintain the optoacoustic probe and the imaging part in the same position during the experiment to visualize dynamic biological events in the region of interest.
7. Inject a contrast agent to track its dynamic distribution in the region of interest.
   NOTE: In our mouse experiments, Indocyanine Green (ICG) was used for contrast enhancement. As a general guideline, an amount of 10 nmol or 0.4 mg/kg of ICG has to be introduced into the mouse circulation in order to create detectable contrast with multi-spectral optoacoustics *in vivo*.
   NOTE: The contrast agent must be approved for human and/or animal use by the respective authority.

5. Finalizing the Experiment

1. Stop the laser.
2. Remove the optoacoustic probe from the imaged region. For animal study, stop the anesthesia supply.
3. Position the animal under an infrared heater to keep it warm and prevent the contact with other animals until it fully recovered from the anesthesia. Do not leave the animal unattended during recovery from the anesthesia.

6. Off-line Data Processing

1. Load the file(s) containing the acquired optoacoustic signals in the software application used for data processing.
2. Use a reconstruction algorithm to obtain a three-dimensional matrix array corresponding to a volumetric image of the optical absorption for each frame and each wavelength.
   NOTE: For the reconstruction it is preferable to use an algorithm accounting for distorting factors, such as heterogeneities and attenuation in the imaged object, effects of final bandwidth and geometrical shape of the detection elements and light fluence variations, in order to obtain a more quantitative representation of the distribution of the absorbed energy.
3. Use an unmixing algorithm to obtain, from each multi-wavelength frame, a new set of three-dimensional matrix arrays representing the optical absorption for each absorbing substance present in the sample.
4. If needed, further process the matrix arrays representing the optical absorption distribution to facilitate visualization and reading of biologically relevant parameters.

Representative Results

Representative results, demonstrating the capabilities of the described volumetric hand-held optoacoustic probe, are showcased in this section. In all cases, the light fluence on the skin surface was kept below the safety exposure limit of 20 mJ/cm^2 [19].

The performance of the probe in real-time tracking peripheral human vasculature is showcased in **Figure 2**. During the course of this experiment, the probe was slowly scanned along the hand of a healthy human volunteer at a single wavelength of 800 nm with the laser operating at 10 pulses per sec[17], so that real-time visualization of the blood vessels for all scanning positions is achieved. The representative maximum intensity projection (MIP) of the reconstructed images in all three directions are displayed in **Figure 2**. Real-time visualization during the measurement is enabled with a GPU implementation of the filtered back-projection algorithm[17].

The real-time multispectral imaging capacity is showcased in **Figure 3**. Specifically, measurements were performed by scanning the probe along the wrist of a healthy volunteer having blood vessels with different sizes and oxygen saturation levels as well as a melanin-rich skin pigmentation[10]. A 50 Hz pulse repetition rate laser with a wavelength-tuning capability in a per-pulse basis was employed in this case. The laser was tuned to multiple wavelengths between 730 and 850 nm with 30 nm step (5 wavelengths), corresponding to a monotonic decrease in the absorption of melanin, a monotonic increase in the absorption of oxygenated hemoglobin and a characteristic peak in the absorption of deoxygenated haemoglobin. Acquisition of an entire multispectral dataset takes only 100 msec due to the fast-tuning capacity of the laser. The MIP images along the depth direction for 3 different wavelengths, corresponding to the same position of the probe, are displayed in **Figure 3A**. **Figure 3B** shows the unmixed distribution of oxygenated hemoglobin (HbO_2), deoxygenated hemoglobin (HbR) and melanin in red, blue and yellow, respectively, whereas it was further assumed that the absorption was solely due to these three chromophoric components. Thereby, red and blue structures in **Figure 3** most likely represent arteries and veins, respectively, whereas the yellow spot corresponds to skin pigmentation. Strong light absorption by melanin may reduce the applicable depth of penetration for this method in people with dark skin, although further testing is clearly necessary to draw quantitative conclusions.

Figure 4 illustrates the capability of imaging dynamic processes *in vivo*. Herein, the circulation in the middle finger was obstructed by means of a rubber band and released during data acquisition[18]. A sequence of single wavelength images was acquired at 10 frames per sec as determined by the pulse repetition rate of the laser. Four MIP images along the lateral and depth directions spaced by 1 sec are showcased, where the second image corresponds to the instant after the circulation was restored. The wavelength was set to 900 nm, so that amplitude of the optoacoustic signals is increased both with blood volume and blood oxygenation.

Finally, **Figure 5** demonstrates the ability of the introduced system to track perfusion dynamics in a three-dimensional region of a mouse by using ICG as a contrast agent [9]. An eight week-old female nude CD-1 mouse was used for the *in vivo* experiments. The experimental procedure was

in agreement with institutional and Bavarian government rules and regulations. The brain vasculature was imaged by positioning the mouse in a supine position and 2% isoflurane in pure oxygen was used for anesthesia. Vet ointment was used to protect the eyes of the mouse. 10 nmol of ICG diluted in 50 ml of saline was injected 5 sec after starting the optoacoustic data acquisition. The wavelength of the laser was tuned to 730, 760, 800, 850 and 900 nm on a per-pulse basis at a rate of 50 times per sec. For each set of wavelengths, the ICG distribution was unmixed by assuming that the optical absorption is only due to this agent as well as the oxygenated and deoxygenated forms of haemoglobin. The MIP images along the depth direction corresponding to the unmixed ICG distribution for 5 different instants are shown in **Figure 5A** (time after injection is also indicated). The absorption spectrum of ICG in plasma is displayed in **Figure 5B**. This particular experiment demonstrates that the suggested approach is capable of simultaneously rendering truly five-dimensional (*i.e.*, spectrally enriched time-resolved three dimensional) tomographic data, which is subsequently used to reconstruct and spectrally unmix the distribution of various intrinsic chromophores and exogenous agents in real time.

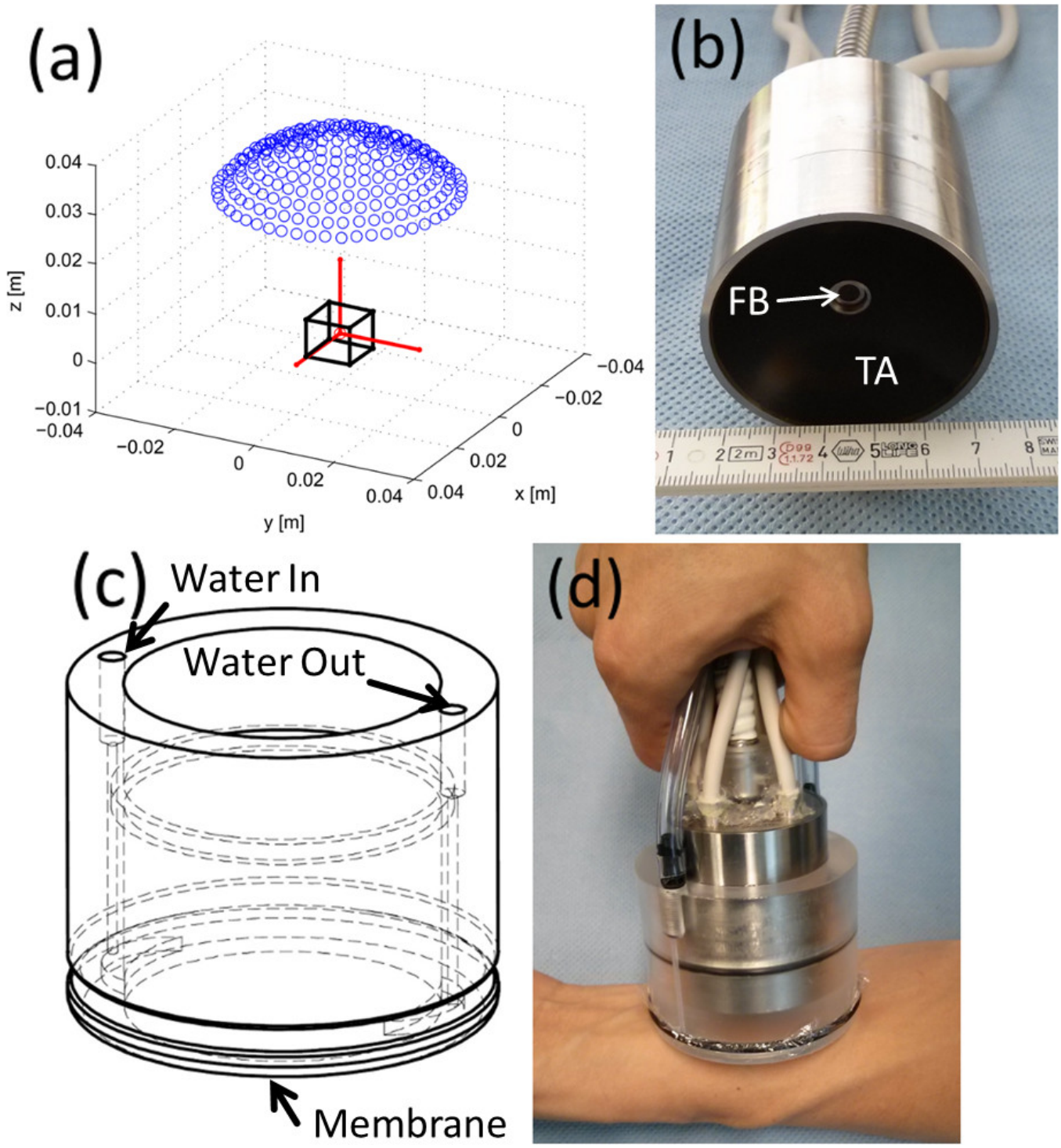

Figure 1: Layout of the hand-held three-dimensional optoacoustic probe. (A) Distribution of the piezoelectric elements (blue dots) with respect to the region of interest (black cube). **(B)** Actual picture of the transducer array (TA) and fiber bundle (FB). **(C)** Water enclosing part. **(D)** Actual picture of the optoacoustic probe as being used in the hand-held operation mode. Please click here to view a larger version of this figure.

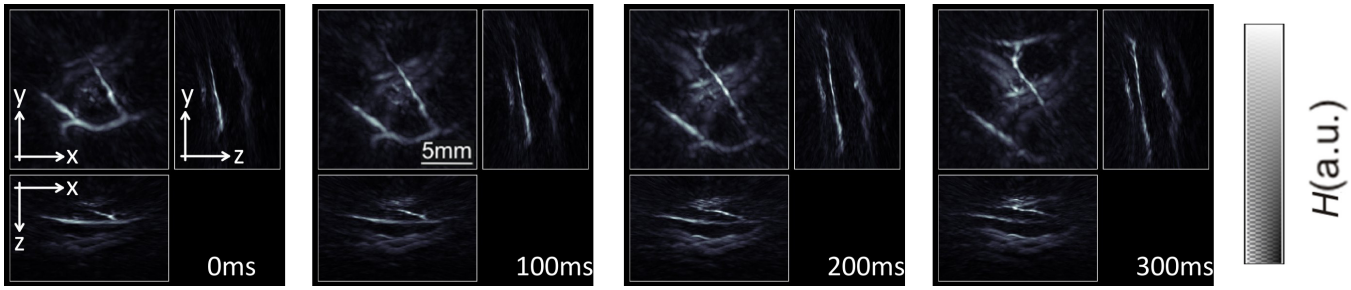

Figure 2: Tracking of peripheral human vasculature. Maximum intensity projection images of optical absorption along the three Cartesian directions for four consecutive images. Here the laser was operated at 10 pulses per second with a wavelength constantly set at 800 nm. The gray-scale color scheme represents intensity of optical absorption *H* in the object in arbitrary units. Please click here to view a larger version of this figure.

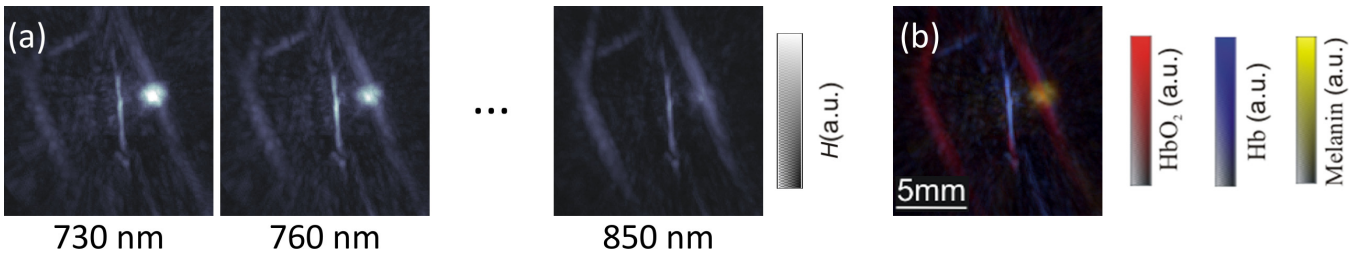

Figure 3: Hand-held imaging of specific endogenous chromophores. (A) Maximum intensity projection images of optical absorption along the depth direction for three different wavelengths corresponding to three consecutive pulses. In this case, the laser operated at 50 pulses per sec (the probe was not moved). **(B)** Spectrally unmixed images showing distribution of oxygenated and deoxygenated hemoglobin and melanin. Please click here to view a larger version of this figure.

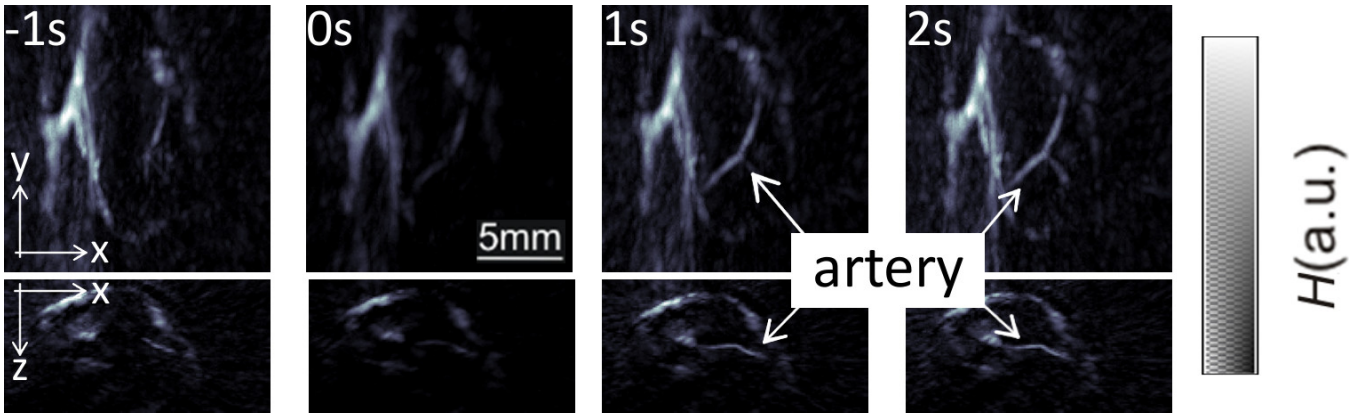

Figure 4: Real-time imaging of blood flow. Maximum intensity projection images of optical absorption along the depth and lateral directions corresponding to four different instants. The circulation in the middle finger was blocked prior to the experiment and released during the experiment (at 0 sec). Please click here to view a larger version of this figure.

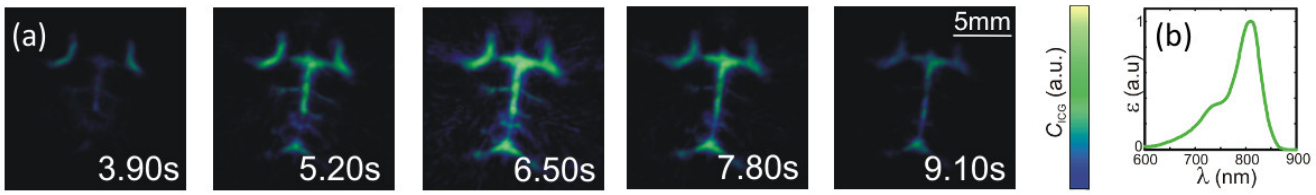

Figure 5: Real-time imaging of the distribution of optical contrast agent in mice. (A) Distribution of the ICG contrast agent (maximum intensity projection along the depth direction) for four different instants after injection of the agent (at 0 sec). **(B)** Extinction spectrum of ICG in plasma. Please click here to view a larger version of this figure.

Discussion

The unique advantages offered by optoacoustic imaging techniques in small animal research have created strong motivation for translating the technology into clinical practice, with a number of diagnostics and treatment monitoring applications envisioned *e.g.*, in breast and skin cancer, inflammation or peripheral vasculature diseases. However, as opposed to mice or smaller animals, which can be surrounded by a sufficient number of illumination sources and detection elements to create an effective tomographic image acquisition geometry, the large dimensions of the human body and limited optical penetration hinder implementation of whole-body optoacoustic tomography similarly to MRI or CT. The

presented hand-held optoacoustic imaging probe is ideal for human imaging as it shares many of the advantages of ultrasonography, such as portable use, high resolution, non-ionizing excitation and real-time capacity. Nevertheless, the optimal hardware design and reconstruction procedures for optoacoustic imaging significantly differ from those commonly used in ultrasound scanners. This is due to fundamental differences between the optimal operational characteristics of the two modalities, such as pulse repetition frequency, amplitude of the detected ultrasonic responses, the underlining signal excitation mechanisms and the resulting image reconstruction approaches. In particular, optoacoustics is inherently a three-dimensional imaging modality as complete volumetric tomographic datasets from the imaged object can in principle be generated with a single interrogating laser pulse, as was also demonstrated in this work. Furthermore, an adaptation of the probe to simultaneously provide ultrasound images can be implemented and remains as one future step in our research agenda.

As compared with other well-established clinical imaging modalities, such as magnetic resonance imaging (MRI) or x-ray computed tomography (CT), optoacoustic tomography is not a whole-body imaging modality but may provide significantly richer and more specific contrast based on light interrogation of tissues. Indeed, endogenous optical absorption contrast does not only deliver high-resolution tissue morphology but also renders functional and potentially targeted molecular information of high importance for clinical decision making. The molecular imaging capacity is further strongly supported by the significantly larger availability of contrast agent approaches of optical imaging methods as compared those available for the other imaging modalities[20,21]. Furthermore, the high temporal resolution of the optoacoustic approach demonstrated here, *i.e.*, high frame rate (real-time) three-dimensional imaging, is not generally available with any other modalities currently in clinical or laboratory use. Finally, simultaneous acquisition of multi-wavelength data brings an additional fifth dimension into the real time volumetric visualization that allows performing true three-dimensional spectroscopic observations of tissues chromophore and specific bio-marker biodistributions.

The potential applications of a three-dimensional optoacoustic hand-held probe are not limited to clinical imaging but it may also represent a highly important tool in biological research with animal models. Indeed, animals larger than mice are generally not suitable to be imaged in a tomographic optoacoustic system and the hand-held approach is probably more convenient. Also, volumetric (three-dimensional) imaging of certain regions in real time with optical contrast and ultrasound resolution represents a unique advantage in the study of drug delivery, hemodynamic changes or pharmacokinetics.

In conclusion, we expect that the introduced methodology for hand-held optoacoustic imaging will prompt clinical translation of the technology and significantly advance pre-clinical and biological research on many frontiers as well.

Disclosures

The authors have nothing to disclose.

Acknowledgements

The research leading to these results has received funding from the European Research Council under grant agreement ERC-2010-StG-260991.

References

1. Stritzker, J., *et al.* Vaccinia virus-mediated melanin production allows MR and optoacoustic deep tissue imaging and laser-induced thermotherapy of cancer. *Proceedings of the National Academy of Sciences of the United States of America.* **110** (9), 3316-3320, doi: 10.1073/pnas.1216916110, (2013).
2. Herzog, E., *et al.* Optical Imaging of Cancer Heterogeneity with Multispectral Optoacoustic Tomography. *Radiology.* **263** (2), 461-468, doi: 10.1148/radiol.11111646, (2012).
3. Johnson, S.P., Laufer, J.G., Zhang, E.Z., Beard, P.C., & Pedley, R.B. Determination of Differential Tumour Vascular Pathophysiology *in Vivo* by Photoacoustic Imaging. *Eur J Cancer.* **48**, S186-S187 (2012).
4. Yao, J.J., *et al.* Noninvasive photoacoustic computed tomography of mouse brain metabolism *in vivo*. *Neuroimage*. **64**, 257-266, doi: 10.1016/j.neuroimage.2012.08.054, (2013).
5. Strohm, E.M., Berndl, E.S.L., & Kolios, M.C. High frequency label-free photoacoustic microscopy of single cells. *Photoacoustics.* **1** (3-4), 49-53, doi:http://dx.doi.org/10.1016/j.pacs.2013.08.003, (2013).
6. Beard, P. Biomedical photoacoustic imaging. *Interface Focus.* **1**, 602-631, doi: 10.1098/rsfs.2011.0028, (2011).
7. Wang, L.H.V., & Hu, S. Photoacoustic Tomography: *In Vivo* Imaging from Organelles to Organs. *Science.* **335** (6075), 1458-1462, doi: 10.1126/science.1216210, (2012).
8. Xiang, L.Z., Wang, B., Ji, L.J., & Jiang, H.B. 4-D Photoacoustic Tomography. *Sci Rep-Uk.* **3** 1113 doi: 10.1038/srep01113, (2013).
9. Buehler, A., Dean-Ben, X.L., Claussen, J., Ntziachristos, V., & Razansky, D. Three-dimensional optoacoustic tomography at video rate. *Optics express.* **20** (20), 22712-22719 doi: 10.1364/OE.20.022712, (2012).
10. Dean-Ben, X.L., & Razansky, D. Adding fifth dimension to optoacoustic imaging: volumetric time-resolved spectrally-enriched tomography. *Light: Science and Applications.* 3 (e137), doi:10.1038/lsa.2014.18 (2014).
11. Fronheiser, M.P., *et al.* Real-time optoacoustic monitoring and three-dimensional mapping of a human arm vasculature. *J Biomed Opt.* **15** (2), 021305, doi: 10.1117/1.3370336. (2010).
12. Buehler, A., Kacprowicz, M., Taruttis, A., & Ntziachristos, V. Real-time handheld multispectral optoacoustic imaging. *Opt Lett.* **38** (9), 1404-1406, doi: 10.1364/OL.38.001404, (2013).
13. Yang, J.M., *et al.* Simultaneous functional photoacoustic and ultrasonic endoscopy of internal organs *in vivo*. *Nat Med.* **18** (8), 1297-1302, doi: 10.1038/nm.2823 (2012).
14. Kruger, R.A., Lam, R.B., Reinecke, D.R., Del Rio, S.P., & Doyle, R.P. Photoacoustic angiography of the breast. *Med Phys.* **37** (11), 6096-6100, doi: http://dx.doi.org/10.1118/1.3497677, (2010).
15. Heijblom, M., *et al.* Visualizing breast cancer using the Twente photoacoustic mammoscope: What do we learn from twelve new patient measurements? *Optics express.* **20** (11), 11582-11597, doi: 10.1364/OE.20.011582, (2012).

16. Dean-Ben, X.L., & Razansky, D. Portable spherical array probe for volumetric real-time optoacoustic imaging at centimeter-scale depths. *Optics express.* **21** (23), 28062-71, doi: 10.1364/OE.21.028062, (2013).
17. Dean-Ben, X.L., Ozbek, A., & Razansky, D. Volumetric real-time tracking of peripheral human vasculature with GPU-accelerated three-dimensional optoacoustic tomography. *IEEE transactions on medical imaging.* **32**(11), 2050-2055, doi: 10.1109/TMI.2013.2272079, (2013).
18. Dean-Ben, X.L., & Razansky, D. Functional optoacoustic human angiography with handheld video rate three dimensional scanner. *Photoacoustics.* **1** (3-4), 68-73, doi: http://dx.doi.org/10.1016/j.pacs.2013.10.002, (2013).
19. *Americal National Standards for the Safe Use of Lasers ANSI Z136.1*. http://www.lia.org/PDF/Z136_1_s.pdf. Americal Laser Institute (2000).
20. Ntziachristos, V., & Razansky, D. Molecular imaging by means of multispectral optoacoustic tomography (MSOT). *Chemical reviews.* **110** (5), 2783-2794, doi: 10.1021/cr9002566, (2010).
21. Luke, G.P., Yeager, D., & Emelianov, S.Y. Biomedical Applications of Photoacoustic Imaging with Exogenous Contrast Agents. *Ann Biomed Eng.* **40** (2), 422-437, doi: 10.1007/s10439-011-0449-4, (2012).

